Zinc finger and SCAN domain-containing 18 suppresses the proliferation, self-renewal, and drug resistance of glioblastoma cells

Yan Wang [a], Jingwei Peng [b], Chenchen Song [a], Yining Yang [a], Tao Qin [c,*]

[a] *The Pediatric Care and Rehabilitation Division at Affiliated Renhe Hospital of China Three Gorges University, Yichang City, Hubei Province, 443000, China*
[b] *The Department of Pediatrics at Affiliated Renhe Hospital of China Three Gorges University, Yichang City, Hubei Province, 443000, China*
[c] *The Department of Radiology and Radiotherapy at Xingshan County People's Hospital, Yichang City, Hubei Province, 443700, China*

ARTICLE INFO

ABSTRACT

Elucidation of cellular and molecular mechanisms key to glioblastoma growth, self-renewal, survival, and metastasis is important for developing novel therapeutic strategies. In this study, the expression and function of zinc finger and SCAN domain-containing 18 (ZSCAN18) in human glioblastoma cell lines were characterized. Compared with normal astrocytes, ZSCAN18 was significantly down-regulated in all tested glioblastoma cell lines, with the LN-229 cell line having the lowest ZSCAN18 expression. Lentivirus-mediated ZSCAN18 overexpression suppressed glioblastoma cell proliferation, sphere formation, and SOX2 and OCT4 expression, implying the negative role of ZSCAN18 in glioblastoma development. ZSCAN18 overexpression enhanced the sensitivity of glioblastoma cells to Temozolomide. The glioblastoma implantation model showed a consistent inhibitory effect of ZSCAN18 on the proliferation and self-renewal of glioblastoma cells *in vivo*. Notably, ZSCAN18 overexpression resulted in the down-regulation of glioma-associated oncogene homolog 1 (GLI1) which is the terminal component of the Hedgehog signaling. Lentivirus-mediated GLI1 overexpression restored the proliferation and promoted the resistance of glioblastoma cells to Temozolomide. However, GLI1 overexpression did not affect the self-renewal of ZSCAN18-overexpressing glioblastoma cells. Taken together, this research uncovers the role of ZSCAN18 in regulating glioblastoma cell growth and maintenance. ZSCAN18 could be a potential glioblastoma biomarker.

1. Introduction

Glioblastoma is the most common primary brain tumor worldwide [1]. Despite current progress in glioblastoma treatments such as surgery, radiotherapy, chemotherapy, and immunotherapy, the prognosis is still poor. Pediatric glioblastoma is a high-grade glioma with different incidences, locations, and consequences [2]. Understanding the crucial molecular mechanisms that regulate glioblastoma proliferation, survival, drug resistance, and metastasis is of great importance for designing novel efficacious therapies against glioblastoma.

Zinc finger and SCAN domain-containing 18 (ZSCAN18), also known as ZNF447, is a member of the Cys2/His2-type (C2H2) zinc

---

finger protein family. The significance of ZSCAN18 to normal tissue development and disease progression is largely unidentified, although interactome analysis suggests it might have DNA-binding transcription regulation activity [3,4]. A previous report states that the *ZSCAN18* gene promoter was frequently methylated in primary renal cell carcinoma samples, and *ZSCAN18* knockdown favors renal cell carcinoma growth [5]. Similarly, the *ZSCAN18* gene is also frequently methylated in gastrointestinal cancers and oropharyngeal squamous cell carcinoma [6,7]. These studies strongly prompt the role of ZSCAN18 as a tumor suppressor. However, to our knowledge, no direct evidence has shown the significance of ZSCAN18 to glioblastoma development. Interestingly, previous studies report the notable effects of other zinc finger proteins on glioblastoma growth and invasiveness [8,9]. Therefore, ZSCAN18 could also regulate glioblastoma development.

Although the relationship between ZSCAN18 and signaling pathways key to glioblastoma growth has not been characterized so far, previous research demonstrates the links between C2H2 zinc finger proteins and these pathways. Zinc finger protein 703 is involved in the modulation of cell proliferation and metastasis of oral squamous cell carcinoma [10]. Zinc finger protein 545 and zinc finger transcription factor 191 affect the Wnt and ERK signal pathways in colorectal cancer and hepatocellular carcinoma [11,12]. Myc-interacting Zinc finger protein 1 regulates the hedgehog pathway to affect tumor growth [13]. ZNF521, another C2H2 zinc finger protein, determines the hedgehog response at the level of transcription [14]. Based on the reports, ZSCAN18 can be thought to impact glioblastoma progression through such pathways. Therefore, we hypothesized that ZSCAN18 might be a tumor suppressor to inhibit the proliferation, self-renewal, and chemoresistance of glioblastoma cells by affecting some malignancy-related signaling pathways. To test this hypothesis, we determined the role of ZSCAN18 in the modulation of proliferation, self-renewal, and drug sensitivity of human glioblastoma cell lines. Our data indicate that ZSCAN18 suppresses glioblastoma growth possibly via down-regulating GLI1 expression.

2. Materials and methods

2.1. Cells

Human glioblastoma cell lines LN-229, U-251, SHG-44, and U87 were purchased from Procell BioTech. All cell lines were authenticated by short tandem repeat (STR) profiling by the suppliers. The cell lines were cultured separately from one another to prevent cross-contamination. Human brain astrocytes were purchased from ScienCell Biotech Co., Ltd. Cells were cultured and passaged in Dulbecco's modified Eagle's medium-F12 (DMEM/F12) containing 10% fetal calf serum (FCS). The cell culture reagents were purchased from Sigma-Aldrich.

2.2. Monolayer culture and proliferation analysis

Glioblastoma cell lines were propagated in 96-well microplates (Corning) at 1×10^3 cells per well for six days. The cell counting kit-8 was purchased from Beyotime Life Technology Inc. and used to treat cells (10 μl/well) for 5 h at indicated time points. The absorbance at 450 nm wavelength was determined on a Tecan Infinite® 200 PRO microplate reader (Tecan).

2.3. Serial sphere culture

Glioblastoma cells were suspended at a density of 5×10^3/ml in neural basal medium containing 10 ng/ml epidermal growth factor (EGF), 20 ng/ml fibroblast growth factor 2 (FGF-2), and 1 mg/ml Heparin (All from Thermo Fisher Scientific). One milliliter of cell suspension was placed in each well of 6-well ultra-Low attachment plates (Corning). The quantity and size of spheres (passage 1) were recorded after 1-week propagation. The spheres were digested with 0.5% Trypsin-EDTA at room temperature for 5 min, followed by gentle pipetting until all spheres become single cells. These single cells were cultured under the same condition as above to generate passage-2 spheres. The above procedures were then repeated to generate passage-3 spheres.

2.4. Temozolomide treatment

Glioblastoma cells were placed in 96-well microplates at 5×10^3 cells per well. Temozolomide (TMZ, T2577-25 MG, Sigma-Aldrich) was added at a final concentration of 50 μM or 100 μM for 48 h. Cell viability was evaluated using the cell counting kit-8 as stated above. In some experiments, cells were dissociated by incubation with 0.5% Trypsin-EDTA at 37 °C for 5 min, followed by flow cytometry analysis of apoptosis and necrosis.

2.5. Immunoblotting

Cells were lysed by RIPA buffer containing protease inhibitors (Beyotime Life Technology Inc) at 4 °C for 30 min followed by centrifugation at $10000 \times g$ for 5 min at 4 °C. A total of 10–20 μg proteins in the lysates were loaded into 12% SDS-PAGE gels for electrophoresis and transfer. The anti-ZSCAN18 monoclonal antibody (MA5-26114, 1:2000, Thermo Fisher Scientific), anti-GLI1 polyclonal antibody (712436, 1:500, Thermo Fisher Scientific), anti-MGMT monoclonal antibody (MA5-13506, 1:100, Thermo Fisher Scientific), anti-SOX2 polyclonal antibody (AF2018-SP, 1 μg/ml, R&D Systems), anti-OCT4 polyclonal antibody (AF1759-SP, 0.5 μg/ml, R&D Systems), anti-S100β monoclonal antibody (AF1820-SP, 0.5 μg/ml, R&D Systems), anti-β-Actin monoclonal antibody (SP124, 1:2000, Abcam).

2.6. Quantitative RT-PCR

RNAs were prepared using the Trizol reagent (Thermo Fisher Scientific) following the vendor's manual. cDNAs were prepared using the protoscript II first strand cDNA synthesis kit (NEB). The powertrack SYBR green master mix (Thermo Fisher Scientific) was used for quantitative PCR on the 7500 fast real-time PCR system (Applied Biosystems™). The mRNA levels of the genes of interest were normalized to β-actin using the $2^{-\Delta\Delta Ct}$ calculation. Primers are demonstrated in Supplementary Tab. 1.

2.7. Flow cytometry assay

The PE-conjugated CD133 antibody (Clone 7), APC-conjugated CD44 antibody (IM7), and PE-conjugated H-2D^d antibody (34-2-12) were obtained from eBioscience. To stain cell surface antigens, 1×10^6/ml cells were stained with 5 μg/ml each antibody at 4 °C for 30 min. For cell cycle analysis, 5×10^5 cells were fixed in 70% ethanol at −20 °C for 1 h. After that, cells were stained with 2 μg/ml Hoechst33342 (Thermo Fisher Scientific) and 4 μg/ml Pyronin Y (Thermo Fisher Scientific) for 1 h. For Ki67 staining, 1×10^6/ml cells were fixed in 3% paraformaldehyde for 15 min, followed by incubation in 90% methanol-PBS for 30 min. Cells were then stained with 5 μg/ml APC-conjugated Ki-67 antibody (SolA15, eBioscience). For apoptosis detection, cells were treated with the Annexin V-APC/PI apoptosis kit (Multisciences) based on the supplier's brochure. A BD FACSCalibur™ Flow Cytometer (BD Biosciences) was used for analysis.

2.8. Lentivirus transduction

The ZSCAN18 lentiviral vector (519630610195) encoding ZSCAN18 and the puromycin-resistant gene, GLI1 lentiviral lector with a CMV promoter-driven GFP reporter (215980610395), and corresponding control vectors were purchased from Abm Inc. Lentiviruses were packaged, purified, and concentrated by Biofavor Biotech Co., Ltd. 1×10^6/ml glioblastoma cells were transduced with relevant lentiviruses at a multiplicity of infection (MOI) of 10 in the presence of 6 μg/ml polybrene (Sigma-Aldrich) overnight. The next morning, the medium was replenished and cells were cultured for another 24 h. After that, puromycin (Sigma-Aldrich) was added at a final concentration of 2 μg/ml to select successfully transduced cells. Two days after puromycin treatment, viable cells were subjected to further experiments.

2.9. Cell migration

3×10^4 LN-229 cells were suspended in serum-free DMEM/F12 and placed on top of a matrigel invasion chamber (BD Biosciences). DMEM/F12 containing 10% FCS was placed in the bottom chamber. After incubation for 12 or 24 h, migrated cells were fixed in 95% ethanol and stained with 0.1% crystal violet. After staining, migrated cells were imaged under a light microscope (Nikon).

2.10. Tumor implantation model

The animal study was approved by the China Three Gorges University Animal Care and Use Committee (Approval# CTGU2019043). The animal experimental procedures complied with theARRIVE guidelines and the National Research Council's grants.nih.gov/grants/olaw/guide-for-the-care-and-use-of-laboratory-animals.pdf" title="https://grants.nih.gov/grants/olaw/guide-for-the-care-and-use-of-laboratory-animals.pdf">Guide for the Care and Use of Laboratory Animals. Eight-week-old male nude mice (BALB/c background) were purchased from Booute Biotechnology Co., Ltd in Wuhan, China. Under anesthesia, 1×10^6 LN-229 cells or U87 cells were suspended in 100 μl of saline and subcutaneously injected into the left posterior flank of each mouse. After 28 days, the mice were euthanized by CO_2 inhalation and the tumors were harvested for size measurement. Tumor growth was monitored every week and computed according to the following equation: volume = (length × width^2)/2.

To isolate tumor cells from tumor implants, the tumor implants were chopped into small pieces with scissors, followed by incubation in DMEM/F12 supplemented 10% FCS, 2 mg/ml collagenase type IV, 2 mM calcium chloride, and 200 U/ml DNase I (All from Sigma-Aldrich.) for half an hour at 37 °C on an orbital shaker. Digested tumors were gently pressed through a 40-μm cell strainer (Falcon) to become single tumor cell suspensions. Single tumor cells were then incubated with the PE-conjugated H-2D^d antibody according to the surface antigen staining protocol, followed by intracellular staining with the APC-conjugated Ki-67 antibody. In some experiments, H-2D^d-positive tumor cells were sorted by a BD FACSAria III cell sorter (BD Biosciences).

2.11. Statistics

All experiments were independently repeated 2 or 3 times. The data were indicated as mean ± standard deviation. Student's t-test or one-way ANOVA with Tukey post hoc test was used for statistical analysis. A P-value less than 0.05 is statistically significant.

3. Results

3.1. ZSCAN18 is down-regulated in glioblastoma cell lines

We analyzed ZSCAN18 expression in normal human cerebral astrocytes and four glioblastoma cell lines. As illustrated in Fig. 1A &

B & Supplementary 1A, normal astrocytes expressed ZSCAN18 while all glioblastoma cell lines significantly down-regulated ZSCAN18 (3.79-fold decrease in LN-229, 1.86-fold decrease in U251, 3.02-fold decrease in SHG-44, and 2.23-fold decrease in U87 compared with normal astrocytes, respectively). Meanwhile, LN-229 expressed the lowest ZSCAN18 in all glioblastoma cell lines. Therefore, LN-229 was used in the following experiments. To determine whether ZSCAN18 is differentially expressed in glioblastoma stem cells and differentiated glioblastoma cells, CD133$^+$CD44$^+$ LN-229 cells and CD133$^-$CD44$^-$ LN-229 cells were sorted for measuring *ZSCAN18* mRNA levels but no significant difference was found (3.18-fold decrease vs 2.75 fold-decrease compared with normal astrocytes) (Fig. 1C & D). We also evaluated ZSCAN18 proteins in LN-229 monolayers and spheres. ZSCAN18 was equally expressed in LN-229 monolayers and spheres (Fig. 1E & Supplementary 1B).

3.2. ZSCAN18 overexpression suppresses LN-229 proliferation in vitro

To determine the function of ZSCAN18, LN-229 cells were transduced with a *ZSCAN18*-encoding lentivirus to induce *ZSCAN18* overexpression followed by puromycin selection. Viable cells were subjected to further experiments after puromycin selection. As illustrated in Fig. 2A & Supplementary Figure 2, compared with LN-229 cells transduced with the control lentivirus without the *ZSCAN18* sequence, ZSCAN18 overexpression was confirmed in LN-229 cells transduced with *ZSCAN18*-encoding lentivirus. Hereinafter, the control LN-229 cells were termed ZS^{lo} cells, meaning cells expressing low ZSCAN18. The ZSCAN18-overexpressing LN-229 cells were termed ZS^{ov} cells. The Pyronin Y and Hoechst 33342 staining indicated that non-transduced LN-229 cells and ZS^{lo} cells had similar cell cycle profiles, while ZS^{ov} cells had fewer cells in both G1 and S-G2M phases (Fig. 2B & C). This suggested slower proliferation of ZS^{ov} cells. The growth curve assay revealed that ZS^{ov} cells grew more slowly than ZS^{lo} cells (Fig. 2D). Spontaneous cell death was not profoundly impacted by ZSCAN18 overexpression because the frequencies of apoptotic cells and necrotic cells were equivalent between ZS^{ov} cells and ZS^{lo} cells (Fig. 2E). No significant differences in the above parameters were found between non-transduced cells and ZS^{lo} cells.

3.3. ZSCAN18 overexpression impedes self-renewal of LN-229 cells in vitro

The serial sphere culture assay was conducted to assess LN-229 self-renewal. Compared with ZS^{lo} cells, ZS^{ov} cells produced fewer and smaller spheres from passage 1 to passage 3, suggesting that LN-229 self-renewal was impeded after ZSCAN18 overexpression (Fig. 3A & B & Supplementary Figure 3). Analysis of stemness markers demonstrated that SOX2 and OCT4 were profoundly reduced (1.73-fold decrease and 2.71-fold decrease, respectively) while S100β, an astrocyte marker, was increased by 1.32 folds in ZS^{ov} cells relative to ZS^{lo} cells (Fig. 3C & D & Supplementary Figure 4). β-III tubulin expression was not affected by ZSCAN18 overexpression (Fig. 3C & D & Supplementary Figure 4). No significant differences in the above parameters were found between non-transduced cells and ZS^{lo} cells.
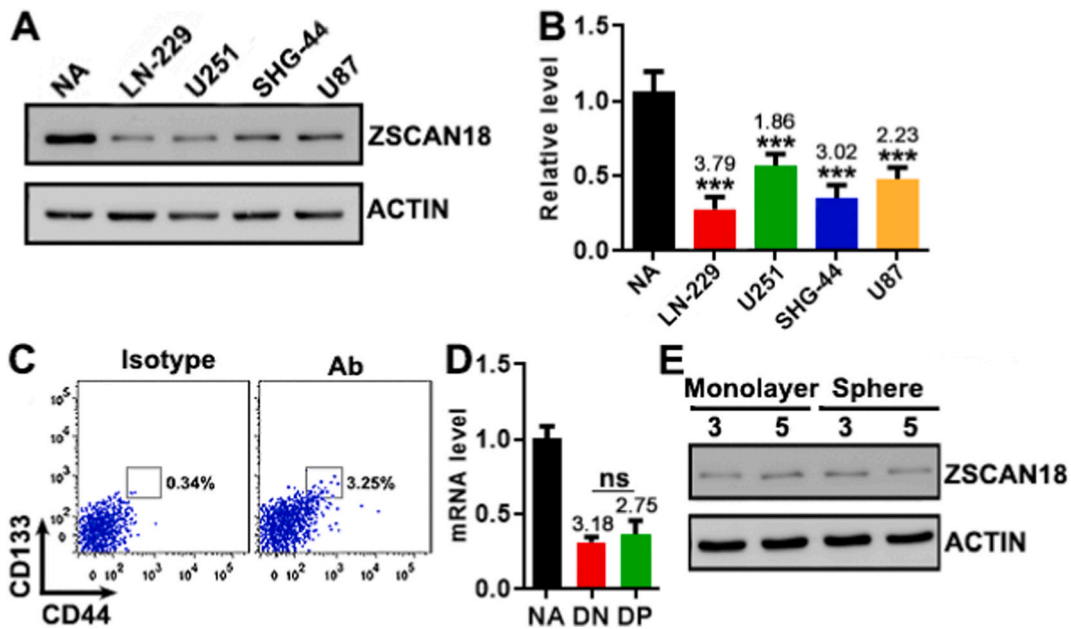

Fig. 1. ZSCAN18 expression in glioblastoma cell lines. (A and B) ZSCAN18 protein in normal astrocytes (NA) and glioblastoma cell lines. Representative blots are shown in (A), and statistics are shown in (B). (C) Flow cytometry dot plots showing CD133$^+$CD44$^+$ LN-229 cells (double positive, DP) and CD133$^-$CD24$^-$ LN-229 cells (double negative, DN). (D) *ZSCAN18* mRNA levels in DN LN-229 cells and DP LN-229 cells. (E) ZSCAN18 protein in LN-229 monolayers and spheres. 3: day 3 culture. 5: day 5 culture. The numbers above the bars indicate fold decreases in ZSCAN18 protein. n = 3 or 6 per group. ***: $p < 0.001$ relative to the NA group. ns: not significant. One-way ANOVA.
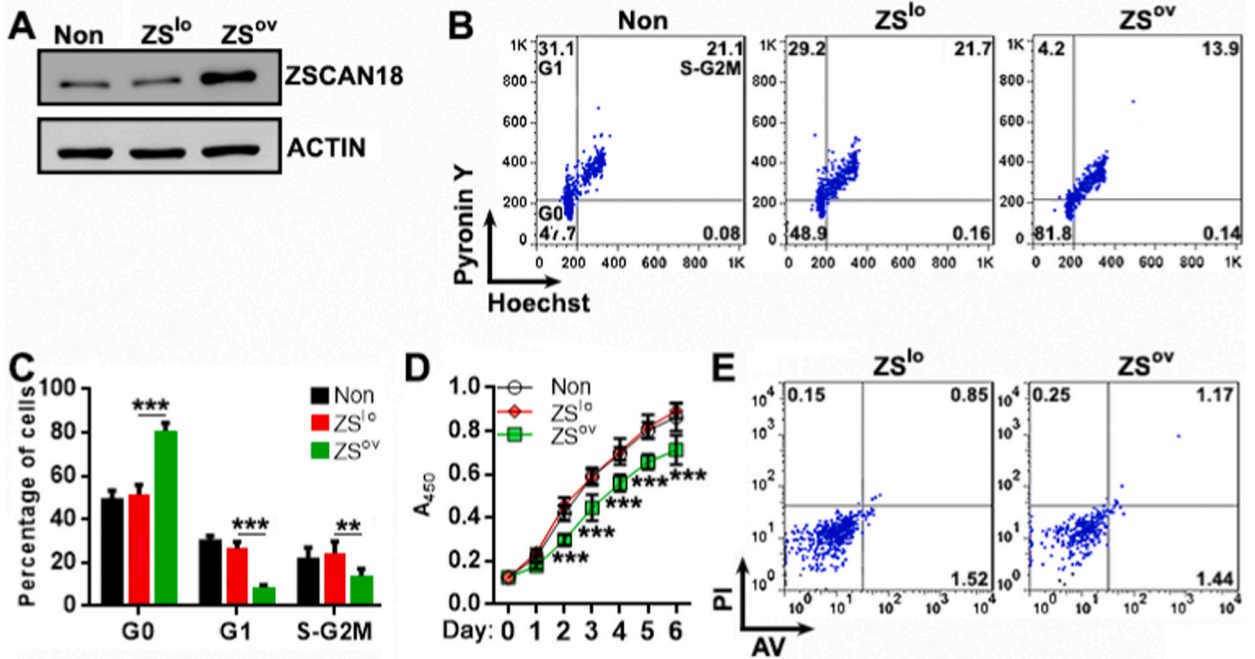
Fig. 2. LN-229 cell proliferation and death after ZSCAN18 overexpression. (A) ZSCAN18 protein in non-transduced LN-229 cells (Non), LN-229 cells transduced with control lentivirus (ZS^{lo}), and LN-229 cells transduced with *ZSCAN18*-encoding lentivirus (ZS^{ov}) on day 2 after puromycin selection. (B & C) Cell cycle detection by Pyronin Y and Hoechst 33342 staining on day 4 after puromycin selection. Representative flow cytometry dot plots are illustrated in (B). Statistics of the frequencies of cells in indicated cell cycle phases are shown in (C). (D) Growth curves indicated as A450 absorbance. (E) Spontaneous apoptosis and necrosis of LN-229 cells on day 4 after puromycin selection. n = 6 per group. **: $p < 0.05$; ***: $p < 0.001$ relative to the ZS^{lo} group. One-way ANOVA.
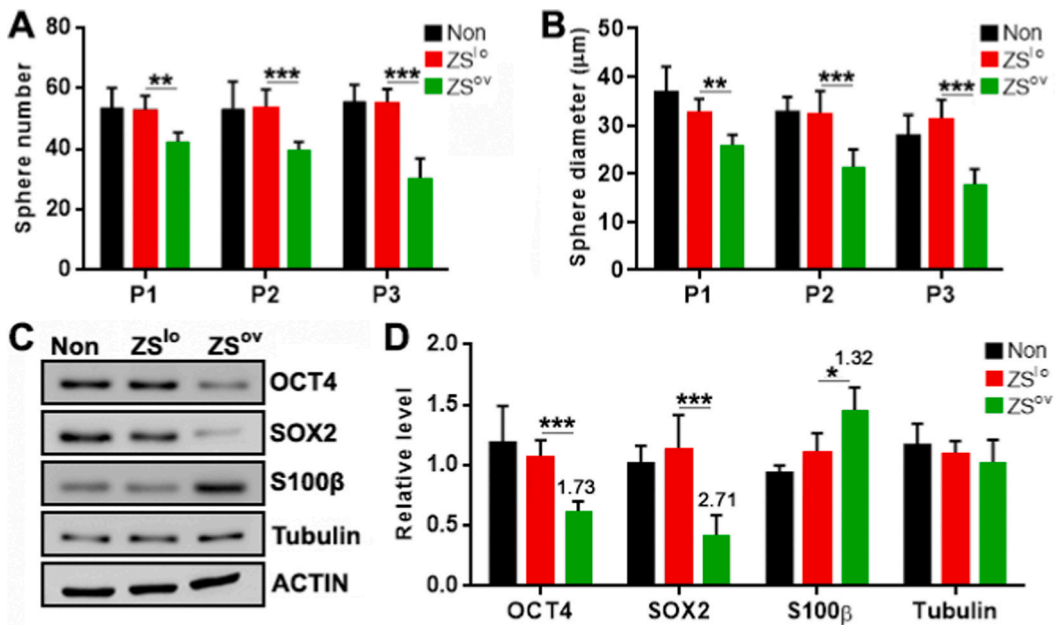

Fig. 3. LN-229 cell self-renewal after ZSCAN18 overexpression. (A) LN-229 cell-derived sphere number at passage 1 (P1), passage 2 (P2), and passage 3 (P3). Non: non-transduced LN-229 cells. ZS^{lo}: LN-229 cells transduced with control lentivirus. ZS^{ov}: LN-229 cells transduced with *ZSCAN18*-encoding lentivirus. (B) Diameters of LN-229 cell-derived spheres. (C & D) Protein levels of indicated markers in P3 spheres. Representative blots are shown in (C), and statistics are shown in (D). The numbers above the bars indicate fold increases or decreases in indicated protein levels. n = 4 to 8 per group. *: $p < 0.05$; **: $p < 0.01$; ***: $p < 0.001$. One-way ANOVA.

3.4. ZSCAN18 overexpression increases sensitivity to TMZ in vitro

TMZ, an anti-glioblastoma agent, induced considerably more apoptosis and necrosis in ZS^{ov} cells compared with ZS^{lo} cells (Fig. 4A and B). Consistently, the viability of ZS^{ov} cells was significantly lower than ZS^{lo} cells after TMZ treatment (Fig. 4C). The Transwell assay was performed to evaluate the invasion capability of LN-229 cells. However, no significant difference in the migration of ZS^{ov} cells and ZS^{lo} cells was observed (Fig. 4D & Supplementary Figure 5). There were no significant differences in the above parameters between non-transduced cells and ZS^{lo} cells.

3.5. ZSCAN18 overexpression has similar effects on other glioblastoma cell lines

To determine whether ZSCAN18 overexpression functions similarly in other glioblastoma cell lines, we conducted the same lentiviral transduction and puromycin selection on U251, U87, and SHG-44 cells. Puromycin-resistant cells, i.e. successfully transduced cells, were used for further analysis. First, ZSCAN18 overexpression was substantiated by profound increases in ZSCAN18 mRNA in ZS^{ov} glioblastoma cell lines compared with ZS^{lo} glioblastoma cell lines (6.9-fold increase in ZS^{ov} U251, 6.2-fold increase in ZS^{ov} U87, and 7.3-fold increase in ZS^{ov} SHG-44) (Supplementary Figure 6A). The proliferation assay indicated slower expansion of ZS^{ov} glioblastoma cell lines relative to ZS^{lo} glioblastoma cell lines, though to different extents (Supplementary Figure 6B). The cell cycle analysis demonstrated fewer G1-phase and S-G2M-phase cells in ZS^{ov} glioblastoma cell lines compared with ZS^{lo} glioblastoma cell lines (Supplementary Figure 6C & 6D). In addition, ZS^{ov} glioblastoma cell lines produced fewer spheres than ZS^{lo} glioblastoma cell lines, especially at passage 2 and passage 3 (Supplementary Figure 7). Similar to ZS^{ov} LN-229 cells, ZS^{ov} U251 cells, ZS^{ov} U87 cells, and ZS^{ov} SHG-44 cells expressed less OCT4 and SOX2 but more S100β than their ZS^{lo} counterparts (Supplementary Figure 8). Furthermore, the viability of ZS^{ov} glioblastoma cell lines was significantly lower than ZS^{lo} glioblastoma cell lines after 100-μM TMZ treatment (Supplementary Figure 9A). Therefore, the roles of ZSCAN18 in tested glioblastoma cell lines seem consistent. Because the O^6-methylguanine-DNA methyltransferase (MGMT) is important for the resistance of glioblastoma to TMZ, we detected MGMT expression in ZS^{lo} and ZS^{ov} glioblastoma cell lines. As shown in Supplementary Figure 9B, all four cell lines were MGMT-deficient regardless of ZSCAN18 overexpression or not. So MGMT might not be involved in the effect of ZSCAN18 in these cells.
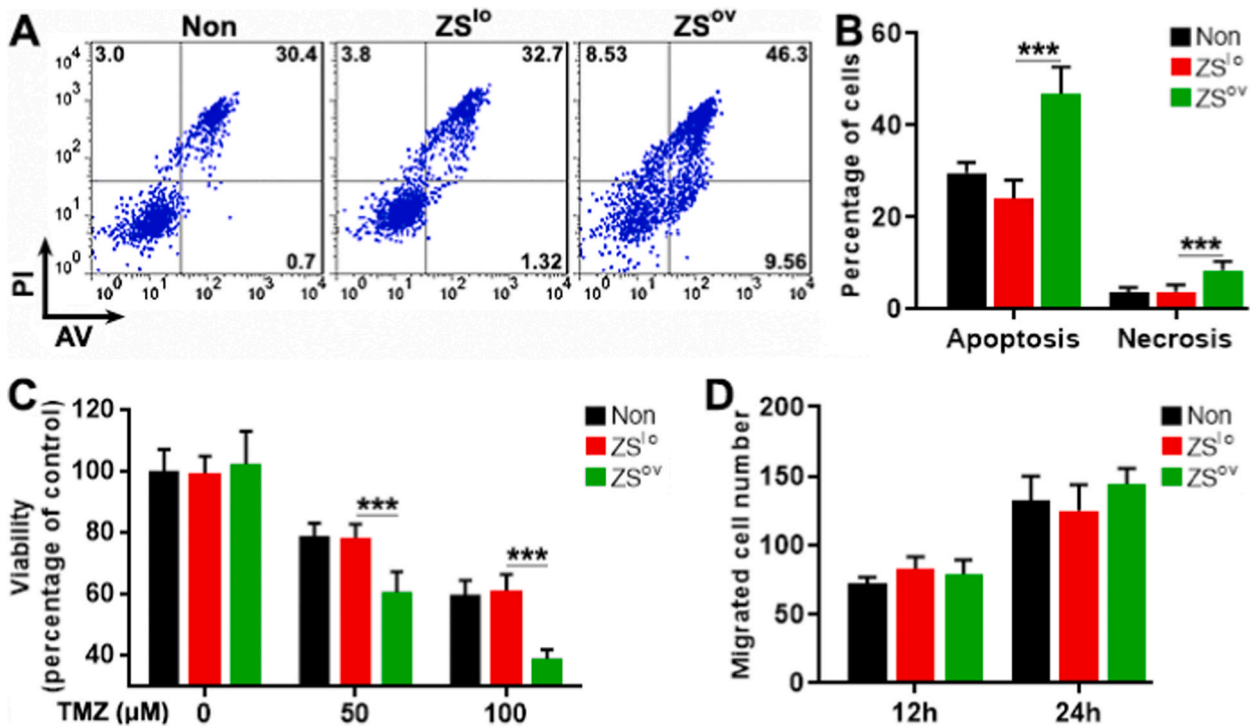

Fig. 4. Cell migration and drug after ZSCAN18 overexpression. (A & B) Apoptosis and necrosis of LN-229 cells after 100 μM TMZ treatment. Non: non-transduced LN-229 cells. ZS^{lo}: LN-229 cells transduced with control lentivirus. ZS^{ov}: LN-229 cells transduced with *ZSCAN18*-encoding lentivirus. Representative plots are illustrated in (A). Statistics of the frequencies of apoptotic and necrotic cells are shown in (B). (C) LN-229 viability after treatment with indicated concentrations of TMZ. (D) Migrated LN-229 cell number after 12-h and 24-h incubation in Transwell plates. n = 5 or 6 per group. ***: $p < 0.001$. One-way ANOVA.

3.6. ZSCAN18 overexpression inhibits LN-229 proliferation and stemness in vivo

To elucidate ZSCAN18 effects *in vivo*, ZS^ov LN-229 cells and ZS^lo LN-229 cells were subcutaneously implanted into nude mice, respectively. The volumes and weights of tumor implants were monitored. ZS^ov cells generated smaller tumor implants compared with ZS^lo cells (Fig. 5A & B & Supplementary Figure 10). The tumor implants were then collected and digested to harvest tumor cells. Mouse cells, which express the murine MHC-I haplotype H-2D^d, were excluded from harvested tumor cells (Fig. 5C). H-2D^d-negative implanted LN-229 cells were then subjected to Ki67 staining. As shown in Fig. 5D and E, the Ki67^+ population in ZS^ov cells was smaller relative to ZS^lo cells. Implanted LN-229 cells were also subjected to Immunoblotting to analyze stemness markers. As shown in Fig. 5F & G & Supplementary Figure 11, OCT4 and SOX2 were decreased (1.9-fold decrease and 2.1-fold decrease, respectively) whereas S100β was increased by 2.5 folds in ZS^ov cell-derived tumor implants, in comparison to ZS^lo cell-derived tumor implants. To determine the sensitivity of implanted LN-229 cells to TMZ, LN-229 cells were sorted from tumor implants and treated with 100 μM TMZ for 48 h. As shown in Fig. 5H and I, TMZ induced comparable apoptosis and necrosis in non-transduced cells and ZS^lo cells. Of note, TMZ induced more apoptosis and necrosis in ZS^ov cells compared with ZS^lo cells.

We also subcutaneously implanted ZS^ov U87 cells and ZS^lo U87 cells in nude mice. ZS^ov U87 cells generated smaller tumor implants than ZS^lo U87 cells *in vivo* (Supplementary Figure 12A). Besides, ZS^ov U87 cells grow more slowly than ZS^lo U87 cells *in vivo*, as evidenced by less Ki67 expression (Supplementary Figure 12B & 12C). Meanwhile, OCT4 and SOX2 expression was lower (1.7-fold decrease and 1.4-fold decrease, respectively) whereas S100β expression was higher (1.4-fold increase) in ZS^ov U87 cell-derived tumor implants, in comparison to ZS^lo U87 cell-derived tumor implants (Supplementary Figure 12D & 12E).
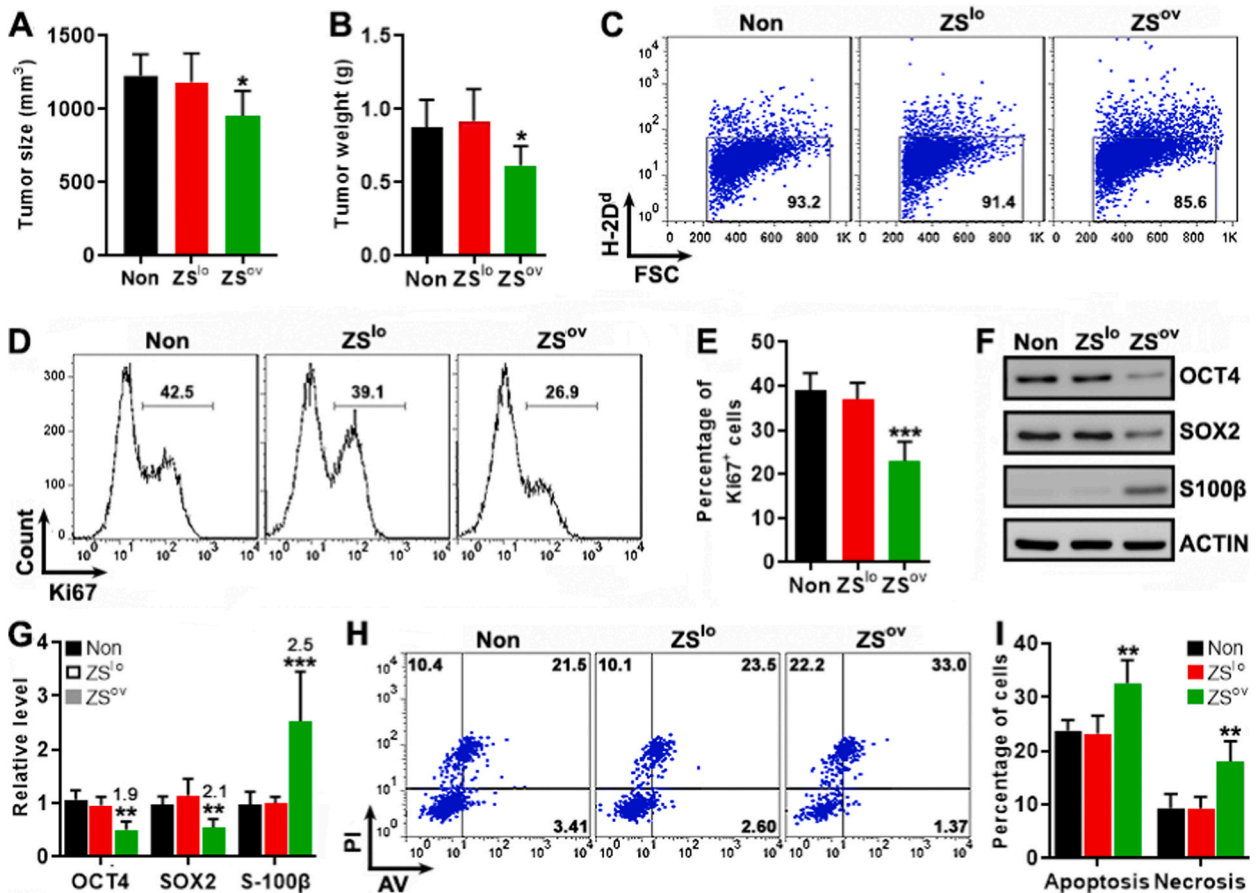

Fig. 5. The effect of ZSCAN18 overexpression *in vivo*. (A) Tumor implant size. Non: non-transduced LN-229 cells. ZS^lo: LN-229 cells transduced with control lentivirus. ZS^ov: LN-229 cells transduced with *ZSCAN18*-encoding lentivirus. (B) Tumor implant weight 28 days after subcutaneous implantation. (C) Exclusion of H-2D^d-positive mouse cells and gating of H-2D^d-negative LN-229 cells by flow cytometry. (D and E) Ki67 staining in LN-229 cells sorted from tumor implants. Representative flow cytometry histograms are illustrated in (D). Statistics of the frequencies of Ki67^+ cells are shown in (E). (F and G) Protein levels of indicated markers in LN-229 cells sorted from tumor implants. Representative blots are shown in (F), and densitometry results are shown in (G). The numbers above the bars indicate fold increases or decreases in indicated protein levels. (H and I) TMZ-induced apoptosis and necrosis of sorted LN-229 cells. Representative plots are illustrated in (I). Statistics of the frequencies of apoptotic and necrotic cells are shown in (I). n = 4 to 8 per group. *: p < 0.05; **: p < 0.01; ***: p < 0.001. One-way ANOVA.

3.7. GLI1 is involved in the ZSCAN18 function

GLI1 is an essential component of the sonic hedgehog pathway. We measured the mRNA levels of molecules key to the sonic hedgehog pathway, including GLI1, SMO, PTCH1, and SHH in LN-229 cells. We found that mRNAs of *GLI1* and *PTCH1* were significantly alleviated (1.96-fold decrease and 2.03-fold decrease, respectively) in ZS^{ov} LN-229 cells relative to ZS^{lo} LN-229 cells, whereas the expression of SMO and SHH was not significantly altered (Fig. 6A). Because GLI1 acts as the transcription factor of PTCH1, we focused on GLI1 in the following analysis. GLI1 down-regulation was substantiated by Immunoblotting (Fig. 6B & Supplementary Figure 13). GLI1 down-regulation was also observed in ZS^{ov} U251 cells (1.99-fold decrease), ZS^{ov} U87 cells (2.05-fold decrease), and ZS^{ov} SHG-44 cells (1.52-fold decrease) compared with their ZS^{lo} counterparts (Supplementary Figure 14). To determine the role of GLI1, ZS^{ov} LN-229 cells were transduced with a lentivirus encoding GLI1 and GFP. More than 85% of ZS^{ov} LN-229 cells were transduced, as shown by the frequency of GFP$^+$ cells (Supplementary Figure 15). GFP$^+$ZS^{ov} LN-229 cells were then sorted for testing their properties. GLI1 overexpression was achieved in transduced ZS^{ov} LN-229 cells (Fig. 6C & Supplementary Figure 16). Hereinafter, GLI1-overexpressing ZS^{ov} LN-229 cells were designated ZS^{ov}-G^{ov} LN-229 cells, whereas ZS^{ov} LN-229 cells transduced with the control lentivirus free of the GLI1 sequence were designated ZS^{ov}-G^{lo} LN-229 cells. ZS^{ov}-G^{ov} LN-229 cells grew faster than ZS^{ov}-G^{lo} LN-229 cells, but still more slowly than ZS^{lo} LN-229 cells (Fig. 6D). ZS^{ov}-G^{ov} LN-229 cells and ZS^{ov}-G^{lo} LN-229 cells formed similar amounts of spheres, suggesting that GLI1 was not essential for self-renewal (Fig. 6E). Impressively, ZS^{ov}-G^{ov} LN-229 cells were more resistant to
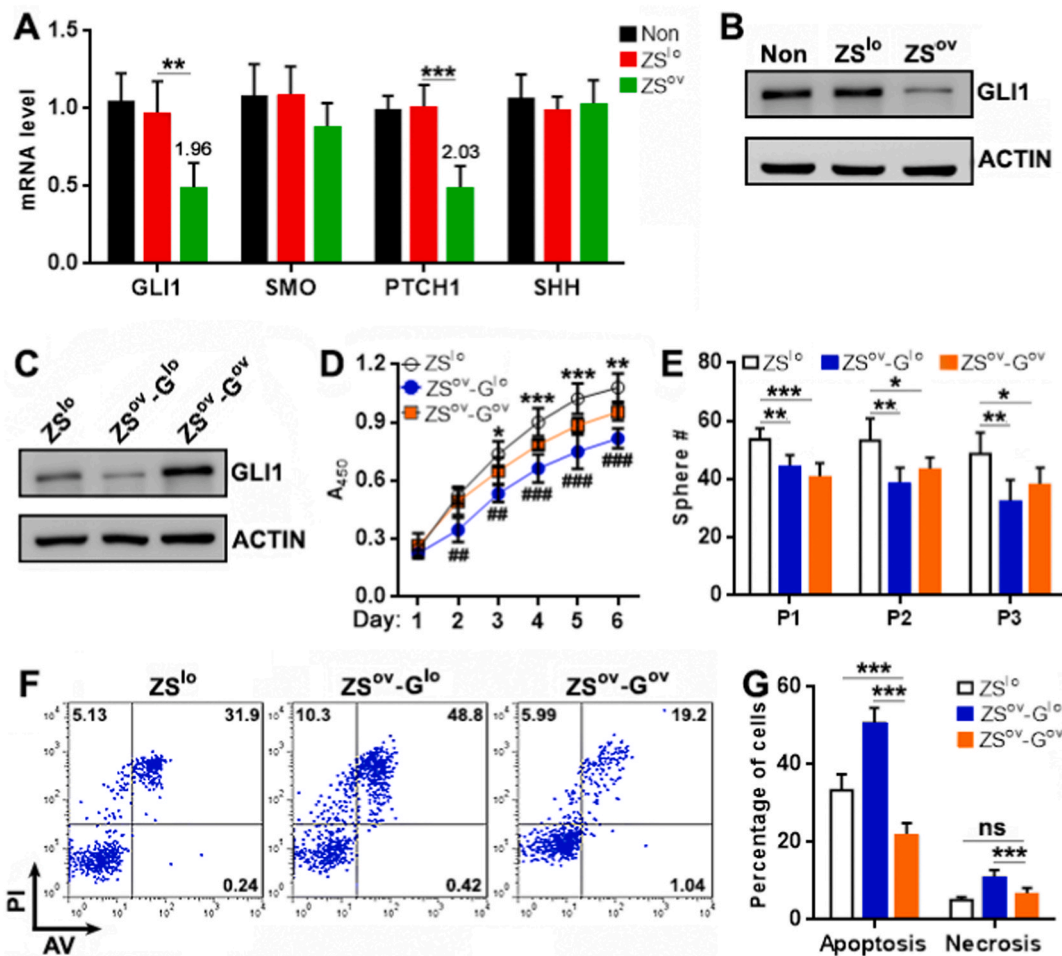

Fig. 6. The significance of GLI1 to ZSCAN18-mediated effects. (A) mRNA levels of indicated sonic hedgehog signaling components in LN-229 cells. Non: non-transduced LN-229 cells. ZS^{lo}: LN-229 cells transduced with control lentivirus. ZS^{ov}: LN-229 cells transduced with *ZSCAN18*-encoding lentivirus. The numbers above the bars indicate fold decreases in the levels of indicated proteins. (B) GLI1 protein in LN-229 cells. The blots represent two independent experiments. (C) GLI1 protein in LN-229 cells on day 2 after secondary lentiviral transduction. ZS^{lo}: ZS^{lo} cells without secondary transduction. ZS^{ov}-G^{lo}: ZS^{ov} cells transduced with secondary control lentivirus. ZS^{ov}-G^{ov}: ZS^{ov} cells transduced with *GLI1*-encoding lentivirus. (D) Growth curves of LN-229 cells. *: $p < 0.05$; **: $p < 0.01$; ***: $p < 0.001$ between the ZS^{lo} group and ZS^{ov}-G^{ov} group. ##: $p < 0.01$; ###: $p < 0.001$ between the ZS^{ov}-G^{lo} group and ZS^{ov}-G^{ov} group. (E) LN-229-derived sphere number at passage 1 (P1), passage 2 (P2), and passage 3 (P3). (F & G) Apoptosis and necrosis of LN-229 cells after 100 μM TMZ treatment. Representative plots are illustrated in (F). Statistics of the frequencies of apoptotic and necrotic cells are shown in (G). n = 5 or 6 per group. ns: not significant. One-way ANOVA.

TMZ than either ZS^{ov}-G^{lo} LN-229 cells or ZS^{lo} LN-229 cells, as evidenced by much fewer apoptotic ZS^{ov}-G^{ov} LN-229 cells after TMZ treatment (Fig. 6F & G). Therefore, GLI1 is involved in ZSCAN18-mediated suppression of proliferation and enhancement of TMZ sensitivity (Fig. 7).

4. Discussion

In the present study, we identified ZSCAN18 down-regulation in various glioblastoma cell lines in comparison to normal astrocytes. Previous studies have shown that the *ZSCAN18* gene is frequently methylated in various tumors [5–7]. DNA methylation can silence genes by interfering with the sequence-specific binding of transcription activators or by producing more general effects on chromatin [15]. In glioblastoma cells, hypermethylation might incur inefficient *ZSCAN18* gene transcription and consequently decreases ZSCAN18. In future studies, it is necessary to determine the methylation status of the *ZSCAN18* gene in both glioblastoma cell lines and clinical specimens.

In humans, the C2H2 zinc finger family members possibly act as transcription factors or co-factors [16]. Besides the DNA-binding ability, C2H2 zinc finger proteins can interact with other signaling molecules or double-stranded RNAs to form transcriptional complexes [16]. ZSCAN18-mediated down-regulation of SOX2 and OCT4, along with the up-regulation of astrocyte marker S100β, strongly suggest that ZSCAN18 is a negative regulator of LN-229 self-renewal. However, it is unknown whether ZSCAN18 suppresses the transcription of SOX2 and OCT4 through direct binding to their gene sequences. It should be necessary to search for ZSCAN18 binding regions in the promoters and enhancers of these genes. Luciferase reporter assays will help display the role of ZSCAN18 in the transcriptional repression of these markers. Since SOX2 and OCT4 are transcriptional factors key to tumorigenesis and drug resistance [17–19], ZSCAN18-mediated down-regulation of SOX2 and OCT4 might mitigate the malignancy of glioblastoma.

In addition, we identified the role of GLI1 in ZSCAN18-mediated effects. GLI1 is a transcriptional factor at the terminal end of the Hedgehog pathway and is involved in the progression of different tumors [20]. GLI1 activates a series of downstream targets including PTCH, GLI2, N-myc, and cyclin D, etc [21]. The Hedgehog signaling and GLI1 positively modulate the proliferation, migration, and survival of glioblastoma cells [22]. Our data suggest that ZSCAN18 suppresses GLI1 expression in LN-229 cells, and GLI1 over-expression counteracts the effect of ZSCAN18 overexpression to partially restore LN-229 cell proliferation and strongly enhance drug resistance. Therefore, ZSCAN18 is likely a direct suppressor of the *GLI1* gene. Our ongoing study is pinpointing the binding site of ZSCAN18 in the GLI1 gene sequence.

Notably, GLI1 overexpression could not increase ZS^{ov} LN-229 cell-derived spheres in the serial sphere culture assay, implying that other proteins rather than GLI1 contribute to ZSCAN18-mediated change in LN-229 self-renewal. Multiple signaling pathways, involving the Ras/MAPK/ERK pathway, Ras/PI3K/AKT pathway, Wnt/β-Catenin pathway, and Notch pathway are critical in the self-renewal of glioblastoma [23–25]. In the future, exploration of the relationships between ZSCAN18 and these pathways would elucidate the exact role of ZSCAN18 in the self-renewal of glioblastoma.

At least half the glioblastoma patients undergoing TMZ treatment developed resistance due to MGMT overexpression [26]. TMZ is an alkylating agent that damages DNA by methylating the O6 position of guanine. MGMT removes alkyl groups from the O^6 position of guanine to induce resistance to TMZ [27]. Of note, our study suggests that ZSCAN18 overexpression increases the sensitivity of these cell lines to TMZ. This effect is related to GLI1 because GLI1 overexpression profoundly enhances the chemoresistance of ZSCAN18-overexpressing glioblastoma cells. Interestingly, past studies indicate that MGMT is a direct transcriptional target of GLI1 by
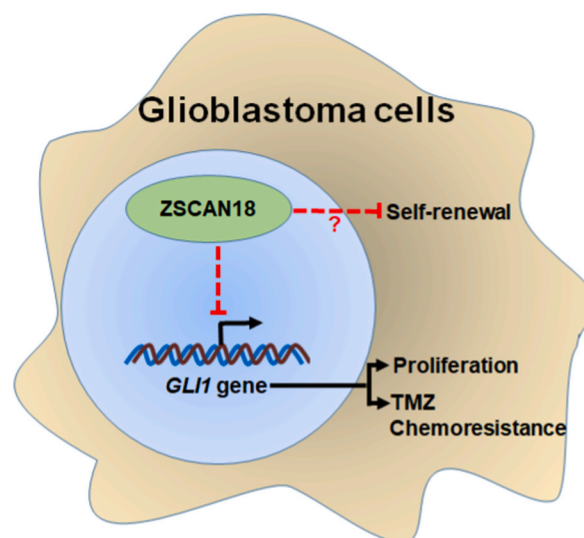

Fig. 7. A possible mechanism underlying the effect of ZSCAN18 on glioblastoma cells. ZSCAN18 might directly suppress the *GLI1* gene expression. Because GLI1 supports glioblastoma cell proliferation and chemoresistance, ZSCAN18 inhibits the proliferation and increases the drug sensitivity of glioblastoma cells. In addition, through an unidentified pathway, ZSCAN18 inhibits the self-renewal of glioblastoma cells.

virtue of GLI-binding sites within its promoter region [28–30], suggesting a potential role of ZSCAN18 in regulating MGMT expression. However, the cell lines used in our study are MGMT-deficient owing to hypermethylation of the *MGMT* gene promoter [31–35]. Therefore, the effect of ZSCAN18 on TMZ resistance may be GLI1-dependent but MGMT-independent. Previous research implies that GLI1 maintains the multidrug efflux activity and decreases nuclear p53 to support the chemoresistance of MGMT-deficient glioblastoma cells such as U87 [36]. So it would be necessary to determine the effects of ZSCAN18 on the multidrug efflux activity and p53 expression/translocation in future studies. In addition, a recent study suggests that Dynein Cytoplasmic 2 Heavy Chain 1 (DYNC2H1), a protein involved in DNA repair, is crucial for TMZ resistance of MGMT-deficient glioblastoma cells [37]. The relationship between ZSCAN18 and DYNC2H1 should also be addressed in the future. Moreover, further investigations are needed to determine if ZSCAN18 regulates MGMT expression in MGMT-expressing glioblastoma cells such as U118MG and U138MG.

The present study suggests that ZSCAN18 is a glioblastoma suppressor. To explore the therapeutic potential of ZSCAN18, it is important to elucidate the upstream regulatory mechanism of ZSCAN18, particularly the negative regulators of ZSCAN18. Small molecules such as synthetic siRNAs and chemical compounds could target these negative regulators to promote ZSCAN18 expression. For example, if the *ZSCAN18* gene is indeed hypermethylated in glioblastoma cells, the methyltransferase(s) responsible for the hypermethylation could be silenced by siRNAs to elevate ZSCAN18 in glioblastoma. Novel nanomaterial-based technology could efficiently assist siRNAs to penetrate the blood-brain barrier [38,39].

This study is limited by the facts that: 1) ZSCAN18 was analyzed only in cell lines. Whether ZSCAN18 has the same expression pattern and function in clinical specimens is unknown. 2) The mechanisms by which ZSCAN18 alters the expression of stemness markers and GLI1 remain unidentified. 3) The cell lines were MGMT-deficient. Whether ZSCAN18 plays the same role in MGMT-expressing glioblastoma is unclear. Regardless of these limitations, this research indicates for the first time that ZSCAN18 acts as a glioblastoma suppressor possibly by down-regulating GLI1. ZSCAN18 could be a biomarker of glioblastoma. Artificial up-regulation or activation of ZSCAN18 could favor glioblastoma therapy.

Ethics approval

The animal study was approved by the China Three Gorges University Animal Care and Use Committee (Approval# CTGU2019043). The study was carried out in accordance with the EC Directive 86/609/EEC for animal experiments.

Author contribution statement

Yan Wang: Performed the experiments; Analyzed and interpreted the data; Wrote the paper.
Jingwei Peng; Chenchen Song: Performed the experiments.
Yining Yang: Analyzed and interpreted the data.
Tao Qin: Conceived and designed the experiments; Wrote the paper.

Data availability statement

Data will be made available on request.

Additional information

Supplementary content related to this article has been published online at [URL].

Declaration of competing interest

The authors declare that they have no known competing financial interests or personal relationships that could have appeared to influence the work reported in this paper.

Appendix. ASupplementary data

Supplementary data related to this article can be found at https://doi.org/10.1016/j.heliyon.2023.e17000.

Abbreviations

ERK   Extracellular signal-regulated protein kinase
GLI1   Glioma-associated oncogene homolog 1
OCT4   Octamer-binding transcription factor 4
PI3K   Phosphoinositide 3-kinase
PTCH1   Protein patched homolog 1
SHH   Sonic hedgehog
SMO   Smoothened
SOX2   SRY-box 2

TMZ   Temozolomide
ZSCAN18   Zinc finger and SCAN domain-containing 18

References

[1] A.C. Tan, D.M. Ashley, G.Y. Lopez, M. Malinzak, H.S. Friedman, M. Khasraw, Management of glioblastoma: state of the art and future directions, CA Cancer J Clin 70 (2020) 299–312.

[2] M. Liu, J.P. Thakkar, C.R. Garcia, T.A. Dolecek, L.M. Wagner, E.V.M. Dressler, et al., National cancer database analysis of outcomes in pediatric glioblastoma, Cancer Med. 7 (2018) 1151–1159.

[3] R. Siddaway, S. Milos, E. Coyaud, H.Y. Yun, S.M. Morcos, S. Pajovic, et al., The in vivo interaction landscape of histones H3.1 and H3.3, Mol. Cell. Proteomics 21 (2022), 100411.

[4] T. Ravasi, H. Suzuki, C.V. Cannistraci, S.Bajic VB. Katayama, K. Tan, et al., An atlas of combinatorial transcriptional regulation in mouse and man, Cell 140 (2010) 744–752.

[5] M.R. Morris, C.J. Ricketts, D. Gentle, F. McRonald, Carli N. Khalili, et al., Genome-wide methylation analysis identifies epigenetically inactivated candidate tumour suppressor genes in renal cell carcinoma, Oncogene 30 (2011) 1390–1401.

[6] H.M. Vedeld, K. Andresen, I.A. Eilertsen, A. Nesbakken, R. Seruca, I.P. Gladhaug, et al., The novel colorectal cancer biomarkers CDO1. ZSCAN18 and ZNF331 are frequently methylated across gastrointestinal cancers, Int. J. Cancer 136 (2015) 844–853.

[7] R.A. Lleras, L.R. Adrien, R.V. Smith, B. Brown, N. Keller C. Jivraj, et al., Hypermethylation of a cluster of Kruppel-type zinc finger protein genes on chromosome 19q13 in oropharyngeal squamous cell carcinoma, Am. J. Pathol. 178 (2011) 1965–1974.

[8] X. Yu, M. Wang, Wu J, Q. Han, X. Zhang, ZNF326 promotes malignant phenotype of glioma by up-regulating HDAC7 expression and activating Wnt pathway, J. Exp. Clin. Cancer Res. 38 (2019) 40.

[9] A. Schuster, E. Klein, V. Neirinckx, A.M. Knudsen, C. Fabian, A.C. Hau, et al., AN1-type zinc finger protein 3 (ZFAND3) is a transcriptional regulator that drives Glioblastoma invasion, Nat. Commun. 11 (2020) 6366.

[10] H. Wang, X. Deng, J. Zhang, Z. Ou, J. Mai, S. Ding, et al., Elevated expression of zinc finger protein 703 promotes cell proliferation and metastasis through PI3K/AKT/GSK-3beta signalling in oral squamous cell carcinoma, Cell. Physiol. Biochem. 44 (2017) 920–934.

[11] S. Xiang, T. Xiang, Q. Xiao, Y. Li, B. Shao, T. Luo, Zinc-finger protein 545 is inactivated due to promoter methylation and functions as a tumor suppressor through the Wnt/beta-catenin. PI3K/AKT and MAPK/ERK signaling pathways in colorectal cancer, Int. J. Oncol. 51 (2017) 801–811.

[12] G. Liu, S. Jiang, C. Wang, W. Jiang, Z. Liu, C. Liu, et al., Zinc finger transcription factor 191. directly binding to beta-catenin promoter. promotes cell proliferation of hepatocellular carcinoma, Hepatology 55 (2012) 1830–1839.

[13] J. Lu, M. Chen, X.R. Ren, J. Wang, H.K. Lyerly, L. Barak, et al., Regulation of hedgehog signaling by Myc-interacting zinc finger protein 1, Miz1. PLoS One 8 (2013), e63353.

[14] S. Scicchitano, M. Giordano, V. Lucchino, Y. Montalcini, E. Chiarella, A. Aloisio, et al., The stem cell-associated transcription co-factor. ZNF521. interacts with GLI1 and GLI2 and enhances the activity of the Sonic hedgehog pathway, Cell Death Dis. 10 (2019) 715.

[15] P.A. Jones, S.B. Baylin, The epigenomics of cancer, Cell 128 (2007) 683–692.

[16] R. Mackeh, A.K. Marr, A. Fadda, T. Kino, C2H2-Type zinc finger proteins: evolutionarily old and new partners of the nuclear hormone receptors, Nucl. Recept. Signal. 15 (2018), 1550762918801071.

[17] A. Liu, X. Yu, S. Liu, Pluripotency transcription factors and cancer stem cells: small genes make a big difference, Chin. J. Cancer 32 (2013) 483–487.

[18] T. Ma, C. Hu, B. Lal, W. Zhou, Y. Ma, M. Ying, et al., Reprogramming transcription factors Oct4 and Sox2 induce a BRD-dependent immunosuppressive transcriptome in GBM-propagating cells, Cancer Res. 81 (2021) 2457–2469.

[19] I.S. Mohiuddin, S.J. Wei, M.H. Kang, Role of OCT4 in cancer stem-like cells and chemotherapy resistance, Biochim. Biophys. Acta, Mol. Basis Dis. 1866 (2020), 165432.

[20] J.T. Avery, R. Zhang, R.J. Boohaker, GLI1: a therapeutic target for cancer, Front. Oncol. 11 (2021), 673154.

[21] E. Mastrangelo, M. Milani, Role and inhibition of GLI1 protein in cancer, Lung Cancer 9 (2018) 35–43.

[22] M. Santoni, L. Burattini, M. Nabissi, M.B. Morelli, R. Berardi, G. Santoni, et al., Essential role of Gli proteins in glioblastoma multiforme, Curr. Protein Pept. Sci. 14 (2013) 133–140.

[23] J.R.D. Pearson, T. Regad, Targeting cellular pathways in glioblastoma multiforme, Signal Transduct. Targeted Ther. 2 (2017), 17040.

[24] N. Rajakulendran, K.J. Rowland, H.J. Selvadurai, M. Ahmadi, N.I. Park, S. Naumenko, et al., Wnt and Notch signaling govern self-renewal and differentiation in a subset of human glioblastoma stem cells, Genes Dev. 33 (2019) 498–510.

[25] H.C. Hung, C.C. Liu, J.Y. Chuang, C.L. Su, P.W. Gean, Inhibition of sonic hedgehog signaling suppresses glioma stem-like cells likely through inducing autophagic cell death, Front. Oncol. 10 (2020) 1233.

[26] S.Y. Lee, Temozolomide resistance in glioblastoma multiforme, Genes Dis 3 (2016) 198–210.

[27] N. Singh, Miner A. Hennis, L. Mittal, Mechanisms of temozolomide resistance in glioblastoma - a comprehensive review, Cancer Drug Resist 4 (2021) 17–43.

[28] J. Cai, J. Chen, S. Zhao, K. Yao, Y. Sun, Y. Li, et al., GANT61. a GLI inhibitor. sensitizes glioma cells to the temozolomide treatment, J. Exp. Clin. Cancer Res. 35 (2016) 184.

[29] J.W. Yoon, R. Gilbertson, S. Iannaccone, P. Iannaccone, D. Walterhouse, Defining a role for Sonic hedgehog pathway activation in desmoplastic medulloblastoma by identifying GLI1 target genes, Int. J. Cancer 124 (2009) 109–119.

[30] K. Wang, D. Chen, Z. Qian, D. Cui, L. Gao, M. Lou, Hedgehog/Gli1 signaling pathway regulates MGMT expression and chemoresistance to temozolomide in human glioblastoma, Cancer Cell Int. 17 (2017) 117.

[31] G. Perazzoli, J. Prados, R. Ortiz, O. Caba, L. Cabeza, M. Berdasco, et al., Temozolomide resistance in glioblastoma cell lines: implication of MGMT. MMR. P-glycoprotein and CD133 expression, PLoS One 10 (2015), e0140131.

[32] N. Gaspar, L. Marshall, L. Perryman, D.A. Bax, S.E. Little, M. Viana-Pereira, et al., MGMT-independent temozolomide resistance in pediatric glioblastoma cells associated with a PI3-kinase-mediated HOX/stem cell gene signature, Cancer Res. 70 (2010) 9243–9252.

[33] M. Chahal, B. Abdulkarim, Y. Xu, M.C. Guiot, J.C. Easaw, N. Stifani, et al., O6-Methylguanine-DNA methyltransferase is a novel negative effector of invasion in glioblastoma multiforme, Mol. Cancer Therapeut. 11 (2012) 2440–2450.

[34] H. Huang, H. Lin, X. Zhang, J. Li, Resveratrol reverses temozolomide resistance by downregulation of MGMT in T98G glioblastoma cells by the NF-kappaB-dependent pathway, Oncol. Rep. 27 (2012) 2050–2056.

[35] J. He, Z. Shan, L. Li, F. Liu, Z. Liu, M. Song, et al., Expression of glioma stem cell marker CD133 and O6-methylguanine-DNA methyltransferase is associated with resistance to radiotherapy in gliomas, Oncol. Rep. 26 (2011) 1305–1313.

[36] J.R. Melamed, J.T. Morgan, S.A. Ioele, J.P. Gleghorn, J. Sims-Mourtada, E.S. Day, Investigating the role of Hedgehog/GLI1 signaling in glioblastoma cell response to temozolomide, Oncotarget 9 (2018) 27000–27015.

[37] G.Z. Yi, G. Huang, M. Guo, X. Zhang, H. Wang, S. Deng, et al., Acquired temozolomide resistance in MGMT-deficient glioblastoma cells is associated with regulation of DNA repair by DHC2, Brain 142 (2019) 2352–2366.

[38] B.A. Eyford, C.S.B. Singh, T. Abraham, L. Munro, K.B. Choi, T. Hill, et al., A nanomule peptide carrier delivers siRNA across the intact blood-brain barrier to attenuate ischemic stroke, Front. Mol. Biosci. 8 (2021), 611367.

[39] Y. Zhou, F. Zhu, Y. Liu, M. Zheng, Y. Wang, D. Zhang, et al., Blood-brain barrier-penetrating siRNA nanomedicine for Alzheimer's disease therapy, Sci. Adv. 6 (2020), eabc7031.